

Green Synthesis of Zinc Oxide Nanoparticles to Study its Effect on the Skin using IR Thermography

Alrabab Ali Zain Alaabedin¹, Basaad Hadi Hamza¹, Aseel Musafa Abdual-Majeed^{1*},
Salim F. Bamsaoud²

¹Department of Physics, College of Science, Mustansiriyah University, 10052 Baghdad, Iraq.

² Department of Physics, Hadhramout University, Yemen.

*Correspondent contact: aseelalaziz@uomustansiriyah.edu.iq

Article Info

Received
11/03/2023

Revised
10/05/2023

Accepted
21/05/2023

Published
30/09/2023

ABSTRACT

The aim of the research is the infrared imaging technique IR Imaging was used to detect temperature changes and their effects on the skin. In this study, ZnO nanoparticles (ZnONPs) were prepared by Green's synthesis method. This method is considered the safest, easiest, and cheapest way to manufacture nanomaterials. The optical and structural properties of ZnO NPs have been studied by various techniques such as UV visible, X-ray diffraction, Field emission scanning electron microscopy, and Transmission electron microscopy. ZnO NPs had a UV- visible absorption peak at around 300 nm. ZnO's average crystallite diameter was calculated to be 15.41 nm using Scherrer's equation, which was derived from the width at half maximum of the peak more intense on the 101 planes at 36.28°. The Field emission scanning electron microscopy data showed that the synthesized ZnO NPs have a consistent shape and size throughout their range, these NPs are characterized by their diameter and were assembled into cylindrical clusters of varying diameters, with an average size of 106. Different magnifications of the ZnO NPs examined by Transmission electron microscopy showed that the majority of the particles were homogeneously scattered. Infrared thermal imaging technique (IRT) is used to clarify the change in temperature with the effect of the substance on the skin. The material was placed on the skin in two ways and put on the rabbit's front and back feet. When mixing the powder material of ZnONPs with distilled water, and mixing the powder material of ZnO NPs with commercial Vaseline, we notice in both cases a temperature rise. The radiance was calculated for each image related to the change of temperature in the band (3-5) μm . The highest value in the range (3-5) μm for image R2 with radiation was (0.9209). The total spectral radioactive emission is proportional to the area under the curves and shifts towards shorter wavelengths with increasing temperature.

KEYWORDS: Green Synthesis; ZnONPs; IR thermography, nanomaterials.

الخلاصة

في هذه الدراسة، تم تحضير الجسيمات النانوية (ZnONPs) بواسطة طريقة Green synthesis. تمت دراسة الخصائص البصرية والهيكلية لـ ZnO NPs من خلال تقنيات مختلفة مثل UV-vis وحيود الأشعة السينية و FESEM و TEM. في طيف امتصاص الأشعة فوق البنفسجية، كانت أعلى ذروة لـ ZnO NPs عند 300 نانومتر. باستخدام معادلة شيرر، قُدِّر متوسط القطر البلوري لـ ZnO بـ 15,41 نانومتر، وقد تم تحديده من العرض عند نصف الحد الأقصى للقمة الأكثر كثافة على المستوى 101 الموجود عند 36,28 درجة، وأظهرت بيانات FESEM أن ZnO NPs المركب له توزيع ومورفولوجيا متجانسة نسبيًا، تتميز هذه NPs بقطرها وتم تجميعها في مجموعات أسطوانية بأقطار مختلفة، بمتوسط حجم 106. أظهرت التكبيرات المختلفة لـ ZnO NPs التي تم فحصها بواسطة TEM أن غالبية الجسيمات كانت مبعثرة بشكل متجانس. تستخدم تقنية التصوير الحراري بالأشعة تحت الحمراء (IRT) لتوضيح التغير في درجة الحرارة بتأثير المادة على الجلد. تم وضع المادة على الجلد بطريقتين ووضعها على قدم الأرنب الأمامية والخلفية. عند مزج مادة مسحوق ZnO NPs بالماء المقطر، وخلط مادة مسحوق ZnO NPs مع الفازلين التجاري، نلاحظ ارتفاعًا في درجة الحرارة في كلتا الحالتين. تم حساب الإنبعثات الطيفية لكل صورة مرتبطة بتغير درجة الحرارة في النطاق (3-5) μm . أعلى قيمة في المدى (3-5) μm ميكرومتر للصورة R2 بعد تشييع النموذج بأشعة IR كانت (0,9209). إجمالي الانبعاث الإشعاعي الطيفي مع المنطقة الواقعة أسفل المنحنيات وينتقل نحو أطوال موجية أقصر مع زيادة درجة الحرارة. الهدف من البحث هو استخدام تقنية التصوير بالأشعة تحت الحمراء IR Imaging للكشف عن التغيرات في درجات الحرارة وتأثيراتها على الجلد.

INTRODUCTION

Zinc oxide is a relatively bio-safe and biocompatible material, making it highly suitable for sensor and transducer applications. Furthermore, nanostructured metal oxides have been found to exhibit attractive nano morphological, functional, biocompatible, non-toxic, and catalytic properties [1-6]. ZnO nanoparticles are in high demand because of their many practical applications in a variety of industries, including UV filters, catalysts, corrosion inhibitors, and antibiotics. In recent years, they have found their primary application in sunscreens as UV-blocking additives. Zinc oxide nanopowders can also be used for things like electrophotography, photo printing, capacitors, protective coatings, antimicrobials, conductive thin films in liquid crystal display screens, solar cells, and blue laser diodes [7]. Synthesis of ZnO NPs via *Salvia officinalis* is a widely adopted technique because many of them are available and can be used easily and safely. The plant extracts contain many bioactive compounds such as alkaloids, flavonoids, terpenoids, tannins, polysaccharides, phenols, and vitamins, as well as many enzymes, amino acids, and proteins. Due to the presence of these bioactive molecules in the plant extract, the synthesis of bioactive ZnO NPs using *Salvia officinalis* is more stable and easier [8].

Without the need for touching the object, infrared thermography can map surface isotherms across specific regions or the entire object [9]. Notably, IRT is a passive (non-invasive, non-radiative) approach, unlike other medical imaging options. Many physical laws underpin the operation of infrared cameras, allowing for the imaging of the temperature distribution on a screen surface while seeing a body at a temperature greater than absolute zero from a particular distance. They include the laws of Stefan-Boltzmann, Wien, Planck, and Kirchhoff. See the theoretical works for a deeper dive into these rules [10-12].

Surface temperatures of all living things are higher than absolute zero (27315 °C), are formed of randomly moving matter, and contain heat due to kinetic energy. The electromagnetic radiation emitted by these substances has two dimensions: wavelength (λ) and strength (Q). The surface temperature of the emitting object determines both the wavelength at which the radiation is strongest and its overall strength. Hence, objects of the same temperature radiate at various wavelengths.

Humans have varying degrees of sensitivity to different parts of the electromagnetic spectrum, but typically we can see wavelengths between 400 and 760 nm [13][14].

The term "body infrared" refers to the limited range of wavelengths between 8 and 12 micrometers that are frequently employed in medical applications [15].

An infrared camera functions by converting the energy of radiation emitted from a body into a temperature reading.

Emissions from objects, reflections from the environment, and atmospheric emissions all contribute to the total amount of energy. A thermal imaging camera's detector sequentially amplifies and transmits an electronic video signal based on the power of incident electromagnetic radiation generated from the body. Each pixel in the thermal image acquired by the infrared camera has a corresponding digital value that is proportionate to the amount of energy received, and this thermal image is known as a thermogram. 30 fps temporal resolution allows dynamic temperature changes to be analyzed. To correctly calculate surface temperatures based on emitted radiation, the emissivity of the object must be known [16][17]. Concerning the spectral domain, human skin is a blackbody radiator with an emissivity of 0.97-0.99 [18] and also functions perfectly as a room-temperature infrared radiator.

Planck's Law states that the electromagnetic waves emitted from a heated object are not a continuous flow, but are composed of discrete units of energy, or quanta and that their magnitude is related to a fundamental physical constant (Planck's constant).

$$R_{\lambda}(T) = \frac{2\pi hc^2}{\lambda^5} \frac{1}{e^{\frac{hc}{kT\lambda}} - 1} \quad (1)$$

Where, R= spectral radiant emittance, ($W\ cm^{-2}\mu^{-1}$)
 $h = 6.62 \times 10^{-34} J \cdot s$, $k =$ Boltzmann's Constant
 $= 1.381 \times 10^{-23} J/Km$

In this study, the infrared imaging technique IR Imaging was used to detect temperature changes and their effects on the skin.

MATERIALS AND METHODS

Materials

10 mL *Salvia officinalis* Extract (1.89g) Zn(NO₃).6H₂O (India) and (0.4 g) NaOH (India) were used as starting materials for the green

synthesis of Ag nanoparticles, Double distilled water was used as the solvent in the experiment.

Preparation of Salvia Officinalis Extract

Salvia officinalis were rinsed with distilled water to remove dust and impurities, finely chopped, and dried for 10 days in the shade. The dried leaves were ground into a fine powder using a domestic grinder. 20g of Salvia officinalis powder was added to 100 ml of deionized water and built at 100 °C for 20 min under magnetic stirring. The solution was cooled down to room temperature, filtered then centrifuged at 3500 rpm for 10 min. The extract will be ready to use.

Synthesis of ZnO Nanoparticles

0.4g NaOH was dissolved in 50 ml of distilled water, placed in a beaker, and stirred over a stirrer until dissolved. $Zn(NO_3)_2 \cdot 6H_2O$ 1.89 is also placed in another beaker with 50 ml of distilled water and placed over a stirrer until completely dissolved. Then 10 ml of the plant extract was added to the NaOH, stirred until uniform, and added drop by drop to the mixture in the second beaker. The material was centrifuged and washed several times with water and ethanol. Finally, the material was dried at 30 °C on a stirrer. A similar result was obtained as in reference [19].

IR Imaging

After we prepared ZnO NPs, it was placed on the skin of the rabbit (rabbit's feet) [all animal handling procedures were conducted under the Care and Use of Laboratory Animals Institute for Laboratory Animal Research Division's ARRIVE (Animal Research: Reporting of In Vivo Experiments) guidelines] [[https:// grants. nih. gov/ grants/law/ guide- for- the- care- and-use-of-laboratory-animals. Pdf](https://grants.nih.gov/grants/law/guide-for-the-care-and-use-of-laboratory-animals.pdf)).

Where we removed the fur from the feet of the rabbit, as shown in Figure 1, then the substance was applied to the skin in two ways. The first method is to mix 0.2 g of ZnO NPs with 2ml of distilled water, and the second method is to mix 0.2g of ZnO NPs with 0.1g of commercial Vaseline. Pictures were taken. Then we repeated the same steps, but this time the skin was irradiated with a heat source that was 75 cm away from the skin, and pictures were taken with the camera every two minutes.



Figure 1: A real picture of a rabbit.

EDX Analysis

Energy-dispersive X-ray analysis (EDX) can be used to determine the elemental makeup of any substance. EDX complements SEM in some ways. When an electron beam with an energy of 10-20keV meets the surface of a conducting sample, X-rays are emitted from the material; the energy of the produced X-rays is dependent on the composition of the sample. Since the X-rays produced by EDX are only produced at a depth of roughly 2 microns, it cannot be classified as a technique for surface science. An image of each component in the sample can be obtained by scanning the material with an electron beam [20].

Field Emission Scanning Electron Microscope

To learn more about the size and shape of nanoparticles, promising methods for examining surface morphology include field emission scanning electron microscopy (FESEM) and high-resolution scanning electron microscopy. Instead of a light beam, electrons are focused on the specimen [20].

Structural Analysis

X-ray diffraction examination is used to ascertain the degree of crystallinity in the material. It can be put to use for other purposes besides just identification. If the sample is a combination, the XRD pattern can be used to calculate the relative amounts of each element. Analysis of the data can also reveal the element's crystallinity, its divergence from the ideal composition, and its structural condition [21].

Transmission Electron Microscopy

The contrast of TEM images differs from that of light microscopic images. When the electron beam

interacts with the material, diffraction occurs rather than absorption. The diffraction intensity changes as a function of the plane's angle relative to the electron beam. If you want the electron to be able to pass through your sample, you'll need to make it into a very thin foil. [22]

UV-Vis Spectroscopy Analysis

To study the optical characteristics of nanomaterials, UV-visible spectrophotometry is employed. Quantum confinement alters the optical characteristics of semiconductor nanoparticles in comparison to their bulk counterparts. The sample is not involved in the path of the reference beam, which travels from the light source to the detector. By interacting with the sample beam, ultraviolet light of varying wavelengths is continually shone on the sample [23][24].

RESULTS AND DISCUSSION

EDX Analysis

This study was used to show the presence of (ZnO) in the mixture in specific ratios. As shown in Figure 2, the analysis listed various patterns for ZnO NPs. The EDX characterization data shown in the table and Figure 2 indicates that the ZnO powder is relatively pure (Zn content: 73.4%, O₂ content: 20.4%). Theoretically, the stoichiometric mass percentages of Zn and O are expected to be 80.3 and 19.7 %, respectively [25]. The composition of zinc is higher than that of synthesized ZnO nanoparticles.

Field Emission Scanning Electron Microscope

Figure 3 shows the surface morphology of a ZnO compound with plant extractants; in Figure 3 (A, B), ZnO is homogeneously distributed and relatively homogeneous in morphology, These NPs are assembled as nanorods. from the entire FESEM image, the average size of nanoparticles is 106 nm is evident

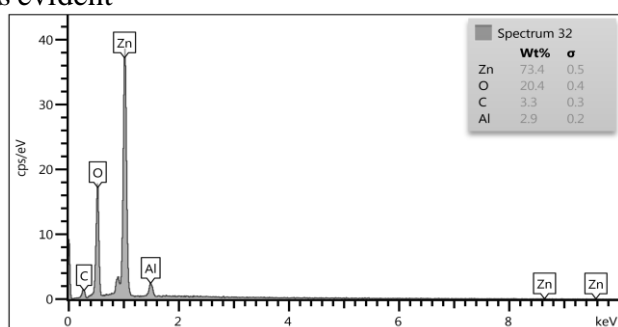


Figure 2: Representing the percentage of metals inset is the atomic weight percentage of elements of the ZnO NPs.

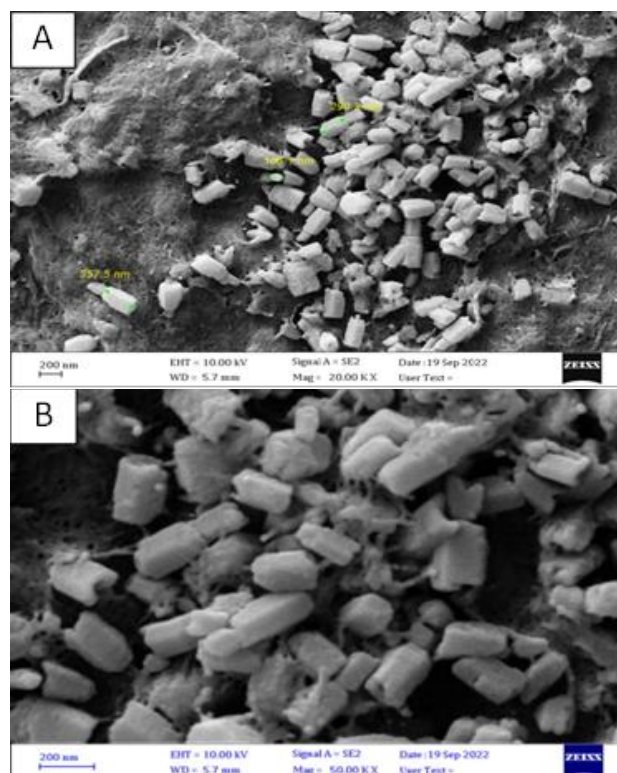


Figure 3: FE-SEM images of ZnO, (A) with scale bar 200 nm with size, (B) with scale bar 200 nm.

Structural Analysis (XRD)

Synthesized ZnO NPs exhibited the X-ray diffraction pattern depicted in Figure 4. The figure displays distinct ZnO peaks, indicating that it is essentially crystalline. The crystalline peaks located at (2θ) peak angles of 31.83°, 34.47°, 36.30°, 47.58°, 56.62°, 62.87°, 67.94°, and 77.35° are respectively (100), (002), (101), (102), (110), (103), (112) to (202) correspond to reflections from the crystal plane. Scherrer's equation was used to calculate an average crystallite diameter of ZnO of 15.41 nm based on the width at half maximum of the peak stronger on the 101 planes at 36.28°.

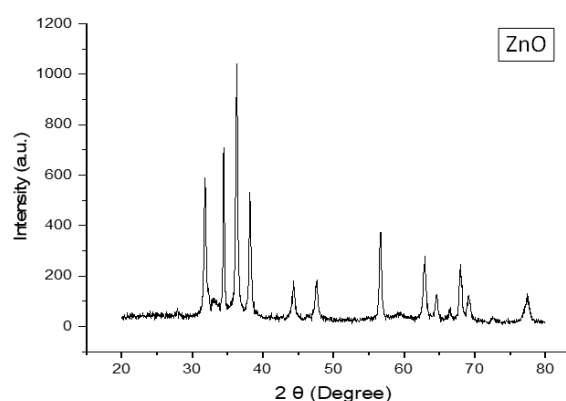


Figure 4: XRD patterns of synthesized ZnO NPs.

Transmission Electron Microscopy

The crystalline characteristics and particle size of produced NPs can be analyzed by TEM. Images taken at various magnifications (1 m, 250 nm, 150 nm, and 60 nm) and analyzed with a JEOL-2100 are presented in Figure 5. The TEM pictures showed a spectrum of particle sizes, from 69 to 145nm.

UV-Vis Spectroscopy Analysis

As shown in Figure 6, the optical absorption spectrum of ZnO nanoparticles was investigated in the range of 300-700 nm at room temperature; the absorption peak of ZnO is at 300 nm.

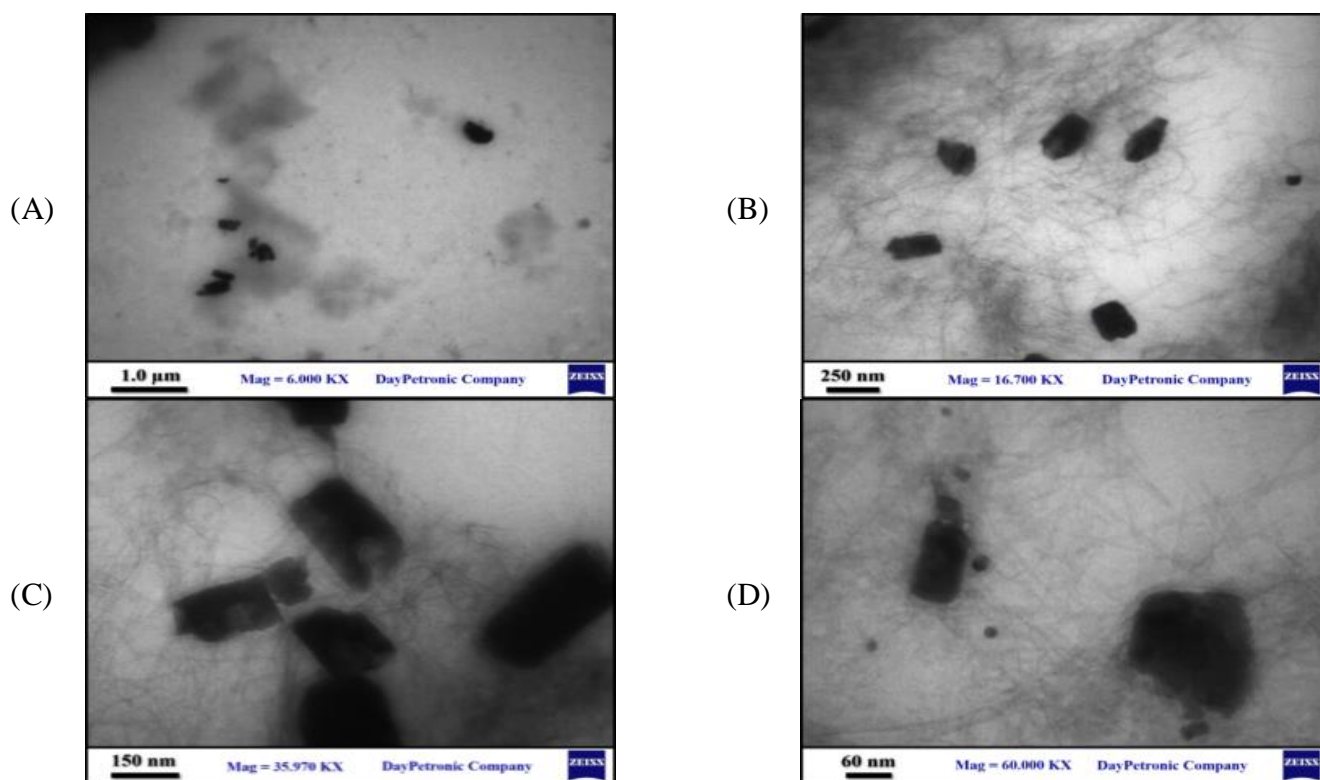


Figure 5: TEM images of ZnO NPs with an inset of different magnifications, (A) with scale bar 1μm, (B) with scale bar 250 nm, (C) with scale bar 150 nm, (D) with scale bar 60 nm.

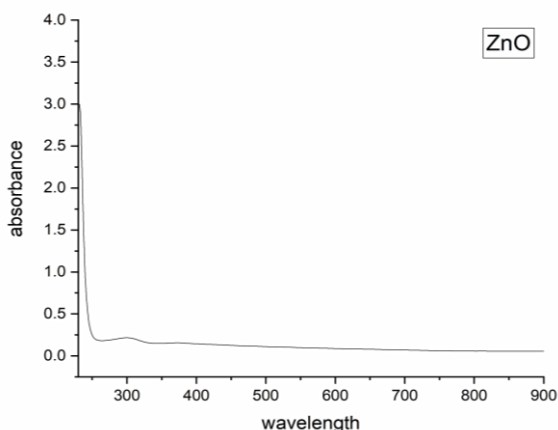


Figure 6: UV-Vis spectra of synthesis the absorption spectrum of ZnO NPs.

IR Thermography Result

The photos were taken in the laboratories of the Department of Renewable Energy of the Ministry of Science and Technology (Baghdad), the IR thermography was used using a thermal camera (Camera Model: Ti10 Fluke. Image Range: 20.6°C to 140.1°C Lens description: 20mm, Accuracy: 5 °C or 5% (whichever is larger) Temperature Sensitivity (NETD): 0.2 °C at 30 °C (200 mK) Visual: We viewed infrared (IR) light from the camera's lens as a temperature gauge, therefore enabled both full-screen IR and picture-in-picture modes. This technique, show the amount of temperature change with the effect of the substance on the skin. Each image was multiplied by a

specific number to enlarge the scale of IR radiance, and the final result was illustrated in Table 1. The

highest value in the range of (3-5) μm for image R2 with radiation was (0.9209).

Table 1: The radiance for each image in the band (3-5 μm), with radiation and without radiation

Radiance ($\text{W}\cdot\text{cm}^{-2}\cdot\mu^{-1}$)									
R1 ($^{\circ}\text{C}$)	R2 ($^{\circ}\text{C}$)	R3 ($^{\circ}\text{C}$)	R4 ($^{\circ}\text{C}$)	R5 ($^{\circ}\text{C}$)	R1 ($^{\circ}\text{C}$)	R2 ($^{\circ}\text{C}$)	R3 ($^{\circ}\text{C}$)	R4 ($^{\circ}\text{C}$)	R5 ($^{\circ}\text{C}$)
44.6-47.3	43.8-46.6	43.1-44.8	41.2-42.3	55.8-59.2	34.7-37.6	43.9-48.5	40.8-47.4	50.0-51.5	55.8-59.2
0.0059	0.0183	0.0635	0.0299	0.0225	0.0007	0.0002	0.0000	0.0595	0.0225
0.0087	0.0277	0.0824	0.0360	0.0307	0.0014	0.0004	0.0000	0.0705	0.0307
0.0127	0.0417	0.1067	0.0432	0.0417	0.0027	0.0008	0.0001	0.0836	0.0417
0.0185	0.0625	0.1378	0.0519	0.0565	0.0051	0.0015	0.0004	0.0990	0.0565
0.0268	0.0931	0.1777	0.0622	0.0761	0.0098	0.0029	0.0011	0.1170	0.0761
0.0387	0.1380	0.2287	0.0745	0.1023	0.0186	0.0054	0.0029	0.1383	0.1023
0.0556	0.2036	0.2938	0.0892	0.1370	0.0349	0.0100	0.0074	0.1632	0.1370
0.0797	0.2990	0.3767	0.1066	0.1828	0.0648	0.0181	0.0187	0.1925	0.1828
0.1136	0.4370	0.4820	0.1274	0.2431	0.1192	0.0325	0.0461	0.2268	0.2431
0.1613	0.6358	0.6156	0.1521	0.3223	0.2171	0.0578	0.1106	0.2669	0.3223
0.2281	0.9209	0.7849	0.1813	0.4259	0.3919	0.1016	0.2591	0.3138	0.4259

After preparing the ZnO NPs, they were placed on the skin of a rabbit, where the rabbit's fur was removed, the material was applied to the skin in two ways: the first method is to mix the powdered ZnO NPs with water and apply it to the skin, as

shown in Figure 7 (A, B, C) the second method is to mix the powdered ZnO NPs with Vaseline, as shown in Figure 7 (D, E). Both methods show an increase in temperature.

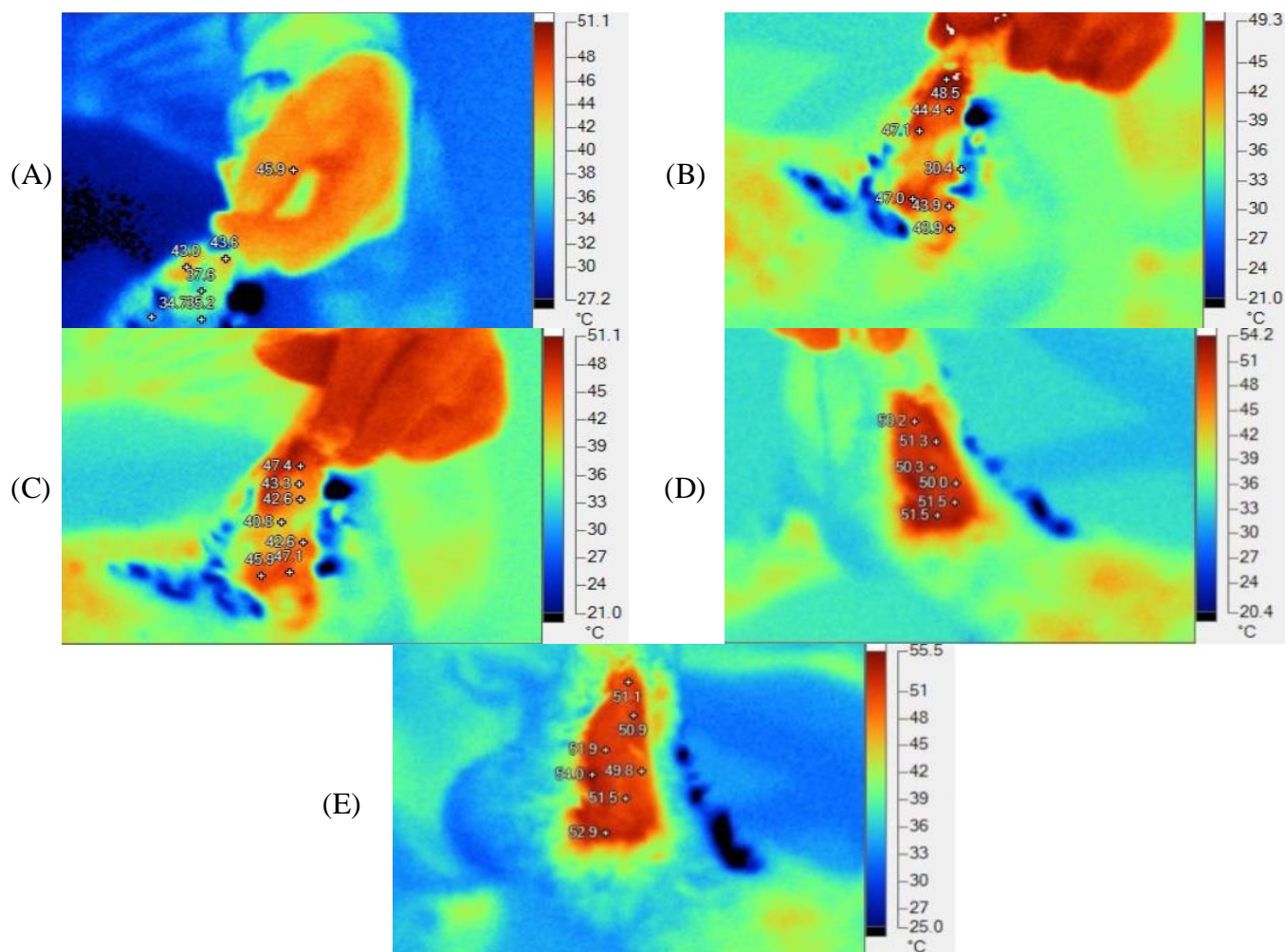


Figure 7: Original photos taken without radiation for rabbit skin, (T1, T2, T3) mix ZnO NPs with water, (T4, T5) mix ZnO NPs with Vaseline.

Figure 8 shows the same two methods of placing substances, Figure 8 (A, B, C) combined with water and Figure 8 (D, E) combined with Vaseline, and it can be seen that the temperature also increases

significantly by placing the radioactive substance after applying the substance to the skin with the two methods.

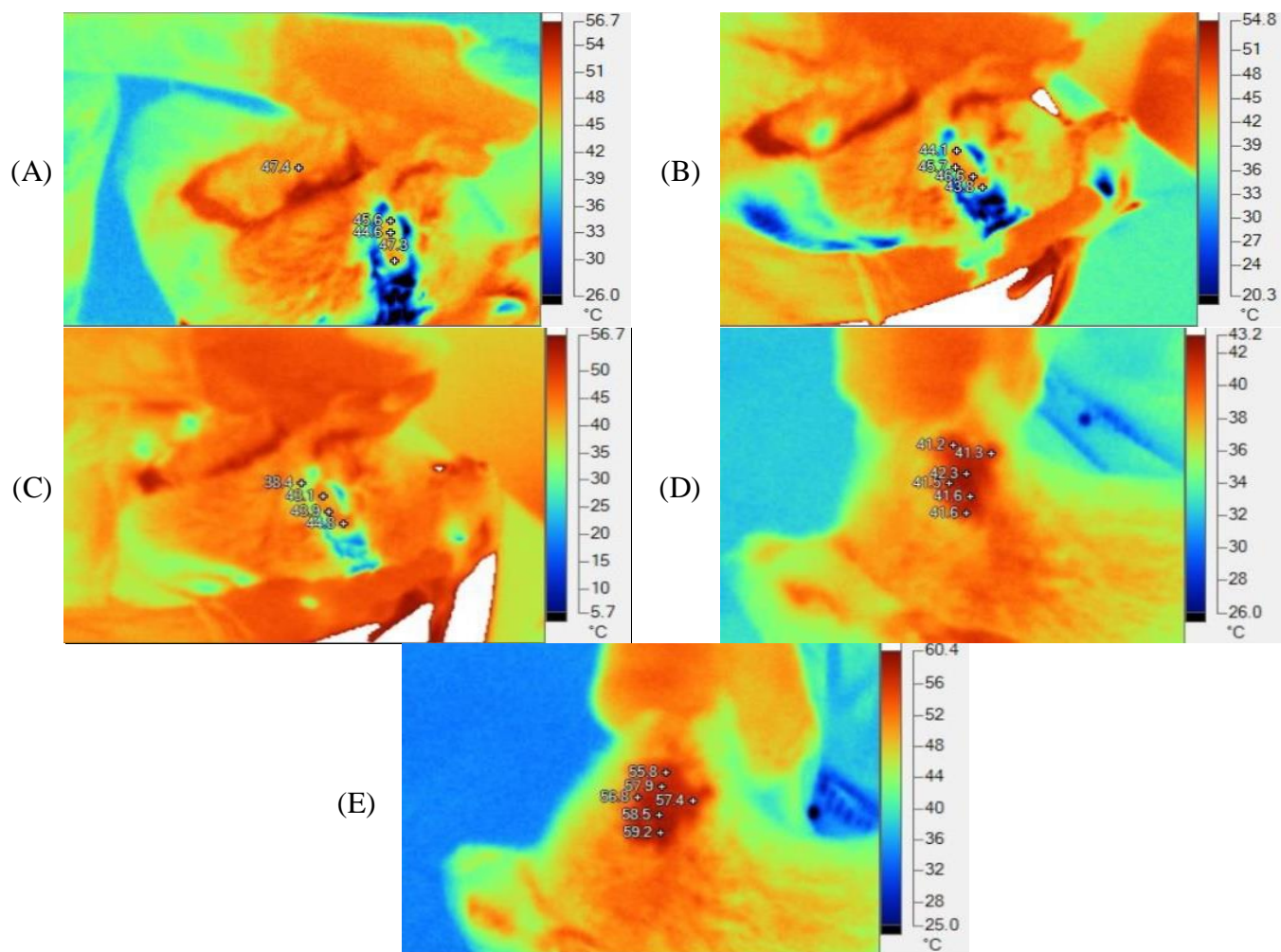


Figure 8: Original photos taken with radiation for rabbit skin, (A, B, C) mix ZnO NPs with water, (D, E) mix ZnO NPs with Vaseline.

In Tables 1, Planck's equation (Eq. 1) was applied. The radiation was calculated for each image based on the temperature change in the 3–5 μm bands, taking into consideration the band in which the camera was operating.

The total radiative emission, which is proportional to the area under the curve, increases rapidly with increasing temperature. The wavelength of the maximum spectral radiation shifts toward shorter

wavelengths with increasing temperature. The higher the temperature, the more spectral radiation is emitted at all wavelengths. When data from line profiles from different temperatures are compared, as shown in Figure 9 (A, B), radial heat diffusion is observed, causing energy to be transmitted to the surrounding regions from the immersed NPs.

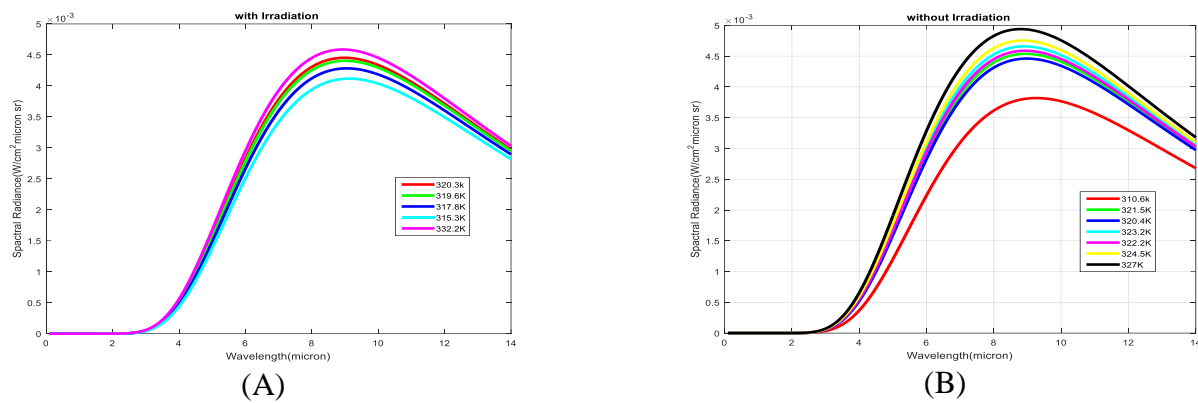


Figure 9: data from line profiles from different temperatures.

CONCLUSION

ZnO NPs were prepared using Green's synthesis method, which is considered the safest, easiest, and most cost-effective approach for manufacturing nanomaterials. The crystal size of the generated ZnO NPs was calculated to be 15.41 nm.

IR thermography is a useful method for studying the material's properties and its impact on the skin. Since the substance resulted in an increase in skin temperature, we recommend that it be blended with other materials if it is to be used as a moisturizer for human skin, such as silver.

ACKNOWLEDGMENTS

The authors would like to extend their gratitude to Mustansiriyah University in Baghdad, Iraq for their assistance with this project.

Disclosure and conflict of interest: The authors declare that they have no conflicts of interest.

REFERENCES

- [1] H. Wahab, A. Salama, A. El-said, O. Nur, M. Willander, and I. Battisha. "Optical, structural and morphological studies of ZnO nano-rod thin film using sol-gel".3, 46-51, 2013.
- [2] D. Look, D. Reynolds, J. Sizelove, R. Jones, C. Litton, and G. Cantwell. "Solid State Commun." 105, 399. 1998.
- [3] P. Yang, H. Yan, S. Mao, R. Russo, J. Johnson, R. Saykally, N. Morris, J. Pham, R. He, and H.-J. Choi, "BControlled growth of ZnO nanowires and their optical properties,"[Adv. Funct. Mater., vol. 12, pp. 323–331, May 2002.
- [4] Q. Wan, Q. Li, Y. Chen, T. Wang, X. He, J. Li, and C. Lin, "B Fabrication and ethanol sensing characteristics of ZnO nanowire gas sensors," Appl. Phys. Lett., vol. 84, pp. 3654–3656, Apr. 2004.
- [5] C. Liu, J. Zapfen, Y. Yao, X. Meng, C. Lee, S. Fan, Y. Lifshitz, and S. Lee, "BHigh-density, ordered ultraviolet light-emitting ZnO nanowire arrays,"[Adv. Mater., vol. 15, pp. 838–841, May 2003."
- [6] H. Kind, H. Yan, B. Messer, M. Law, and P. Yang, "BNanowire ultraviolet photodetectors and optical switches," Adv. Mater., vol. 14, pp. 158–160, Jan. 2002."
- [7] C. Boon, L. Yong and A. Mohammad A review of ZnO nanoparticles as solar photocatalysts: Synthesis, mechanisms and applications". 2018. doi.org/10.1016/j.rser.2017.08.020.
- [8] H. Agarwal, S. Venkat Kumar and S. Rajeshkumar, A review on green synthesis of zinc oxide nanoparticles – An eco-friendly approach" 2017. doi.org/10.1016/j.refit.2017.03.002
- [9] C. Hildebrandt, K. Zeilberger, E. Francis, J. Ring, C. Raschner "The application of medical infrared thermography in sports medicine. In An International Perspective on Topics in Sports Medicine and Sports Injury;" Zaslav, K.R., Ed.; Intech Open: London, UK, Green Version, 2012.
- [10] W. Minkina, "Theoretical basics of radiant heat transfer—Practical examples of calculation for the infrared (IR) used in infrared thermography measurements. Quant. Infrared Thermogr." J. 18, 269–282. 2021.
- [11] J. Speakman, S. Ward," Infrared thermography: Principles and applications. Zoology " 101, 224–232. 1998.
- [12] R. Vardasca, L. Vaz, J. Mendes, "Classification and decision making of medical infrared thermal images. In Lecture Notes in Computational Vision and Biomechanics; Springer." Berlin/Heidelberg, Germany, Volume 26, pp. 79–104. 2018.
- [13] A. Batista-Leyva, "Radiometry and photometry: Two visions of one phenomenon." Rev. Cub. Fis. 36, 66–72. 2019. http://orcid.org/0000-0003-4317-0360
- [14] C. Meola."Origin and Theory of Infrared Thermography. Infrared Thermography: Recent Advances and Future Trends". Bentham Science; New York, NY, USA: 2012.
- [15] H. Qi, N. Diakides," Infrared Imaging in Medicine"; CRC Press: Boca Raton, FL, USA, ISBN 9780849390272. 2007. https://doi.org/10.3390/app12094302
- [16] C. Pereira, X. Yu, S. Dahlmanns, V. Blazek, S. Leonhardt, D. Teichmann, "Infrared thermography. In Multi-Modality Imaging; Springer International"

- Publishing: Cham, Switzerland, pp. 1–30. ISBN 9783319989747. 2018.
- [17] B. Hadi and H. Salh, " Improved Detector Performance Rendering in the Optical Spectral Ranges to Provide Accurate Image", *Mustansiriyah Journal of Science* ISSN: 1814-635X (print), ISSN:2521-3520 .2019. <https://doi.org/10.23851/mjs.v29i4.341>
- [18] J. Stekete, "Spectral emissivity of skin and pericardium". *Phys. Med. Biol.* 18, 686–694. 1973.
- [19] S. Faraj and M. Abdullah, " Effect of silver nanoparticles prepared using sage leaf extract. *Azadirachta indica* and *Prosopis juliflora* in germination and seedling growth *Pepo Cucurbita zucchini* plant and its growth. 2017.
- [20] B. Lewczuk and N. Szyryńska , " Field-Emission Scanning Electron Microscope as a Tool for Large-Area and Large-Volume Ultrastructural Studies" 2021. <https://doi.org/10.3390/ani11123390>
- [21] W. Bragg. "The structure of some crystals as indicated by their diffraction of X-rays. *Proc R Soc Lond*"; A89(610):248–77. 1913.
- [22] P. Werner, S.Eichler, G.Mariani, R.Kogler, and W. Skorupa " Investigation of CxSi defects in C implanted silicon by transmission electron microscopy." *Appl Phys Lett*, 70:252–4. 1997.
- [23] G. Verma and M. Mishra. " DEVELOPMENT AND OPTIMIZATION OF UV-VIS SPECTROSCOPY - A REVIEW.2018. DOI: 10.20959/wjpr201811-12333.
- [24] P.Mulvaney ."Surface plasmon spectroscopy of nanosized metal particles. *Langmuir*";12(3):788–800. 1996.
- [25] A. Bari, M. Shinde, D. Vinita and L. Patil, "Effect of Solvents on the Particle Morphology of Nanostructured ZnO". *Indian Journal of Pure & Applied Physics*, 47, 24-27. 2009. <http://nopn.niscpr.res.in/handle/123456789/3142>.

How to Cite

A. A. Z. . Alaabedin, B. H. . Hamza, A. M. A.-M. Abdual-Majeed, and S. F. . Bamsaoud, "Green Synthesis of Zinc Oxide Nanoparticles to Study its Effect on the Skin using IR Thermography", *Al-Mustansiriyah Journal of Science*, vol. 34, no. 3, pp. 115–123, Sep. 2023.

